

# Tiered Reward Functions: Specifying and Fast Learning of Desired Behavior

Zhiyuan Zhou<sup>1,2</sup>, Shreyas Sundara Raman<sup>2</sup>, Henry Sowerby<sup>2</sup>, Michael Littman<sup>2</sup>,

## Abstract

Reinforcement-learning agents seek to maximize a reward signal through environmental interactions. As humans, our job in the learning process is to design reward functions to express desired behavior and enable the agent to learn such behavior swiftly. In this work, we consider the reward-design problem in tasks formulated as reaching desirable states and avoiding undesirable states. To start, we propose a strict partial ordering of the policy space to resolve trade-offs in behavior preference. We prefer policies that reach the good states faster and with higher probability while avoiding the bad states longer. Next, we introduce Tiered Reward, a class of environment-independent reward functions and show it is guaranteed to induce policies that are Pareto-optimal according to our preference relation. Finally, we demonstrate that Tiered Reward can lead to fast learning by evaluating on several environments using multiple tabular and deep reinforcement-learning algorithms.

## 1 Introduction

Reinforcement learning (Sutton and Barto 1998), aka RL, is concerned with the problem of learning to behave to maximize a reward signal. In biological systems, this reward signal is considered to be the organism’s motivational system, using pain and pleasure to modulate behavior. In engineered systems, however, rewards must be selected by the system designer. We view rewards as a kind of programming language—a specification of the agent’s target behavior (Littman et al. 2017). As arbiters of behavior correctness in the learning process, humans bear the responsibility of authoring this program.

There are two essential steps in designing reward functions. First, one must decide what kind of behavior is desirable and should be conveyed. Then, there’s the choice of reward function that induces such behavior.

In this paper, we look at a specification language that allows for the expression of desirable states (goals and subgoals) and undesirable states (obstacles). Even in this simple setting, providing precise trade-offs is difficult. Is it better for an agent to increase the chance of getting to the goal by 5% if it also incurs 8% higher probability of hitting an

obstacle? Is it better to increase by 50% the probability of getting to a goal if the expected time of getting there also increases by 20%? There is no universal preference over behavior and having to explicitly write down all possible trade-offs is challenging. Even if the reward designer has a way of expressing preferences for all possible exchanges, it can be difficult, or even impossible, to design a reward function that captures them without prior knowledge of the environment.

## Favorable Policies

In the goal–obstacle class of tasks we consider, preferences over policies are simplest in the deterministic setting. We imagine all states are either goal states, obstacle states, or neither (background states). All goal states and obstacle states are absorbing. Preferences in deterministic environments form a total order: reaching the goal is better than reaching the obstacle; if the policy reaches the goal, faster is better; if the policy reaches the obstacle, avoiding it longer is better.

As pointed out before, preferences are less clear in a stochastic setting because there can be trade-offs between different outcomes and their probabilities. However, some comparisons are arguably clear cut. Informally, if one policy induces uniformly better outcomes than another—being more likely to reach a goal and doing so faster, being less likely to reach an obstacle and getting there more slowly—we prefer such a policy. If the policies can’t be directly compared, we propose to be indifferent between them. Thus, we replace the standard reinforcement-learning notion of optimality with Pareto-optimality (Mornati 2013)—seeking a policy that is either preferred or incomparable to every other policy. Pareto-optimal policies are commonly adopted in the subfield of multiobjective RL (Vamplew et al. 2011).

## Reward Design

Policies in general are hard to express through reward functions (Amodei and Clark 2016), and some are even impossible to convey with a Markov (state–action-based) reward (Abel et al. 2021). Even when policies are expressible, designing bad reward functions can lead to undesirable or dangerous actions (Amodei and Clark 2016), easy reward hacking (Amodei et al. 2016), and more. We seek to design good reward functions, which can be characterized by many

<sup>1</sup> UC Berkeley <sup>2</sup> Brown University. Correspondence to: zhiyuan.zhou@berkeley.edu. Code for the paper can be found at <https://github.com/zhouzypaul/tiered-reward>

properties, such as interpretability and learning speed (Dev-  
idze et al. 2021). But the most important property a reward  
function must have is to guarantee the adoption of a desired  
policy. As we will show later in Section 5, even intuitively  
correct reward designs can lead to suboptimal policies.  
To hedge against this, we introduce a tiered reward struc-  
ture that is guaranteed to induce Pareto-optimal policies.  
Intuitively, we partition the state space into several tiers,  
or goodness levels. States in the same tier are associated  
with the same reward, while states in a more desirable tier  
are associated with a proportionally higher reward. We  
prove that these tiered reward structures, with the proper  
constraints between reward values, induce Pareto-optimal  
behavior and empirically show that they can lead to fast  
learning.

Our contribution is threefold: First, we define a prefer-  
ence over the entire policy space via a strict partial ordering  
on outcomes. Then, we introduce a class of environment-  
independent tiered reward structure that provably induce  
Pareto-optimal policies with respect to this preference  
ordering. Finally, we demonstrate these tiered reward  
functions can lead to fast learning in both tabular and deep  
RL settings.

## 2 Related Work

There are many papers that deal with specifying behav-  
ior through rewards. Reward machines (Icarte et al. 2018,  
2022) are finite state machines that compose reward func-  
tions and allow different rewards to be delivered dependent  
on the agent’s trajectory. They reveal the structure of the  
reward function to the RL agent to support decomposition  
of complex tasks. Our focus on how to provide incentives  
for specific outcomes is complementary and the two ap-  
proaches can be used in concert. Temporal logic based lan-  
guages (Littman et al. 2017; Camacho et al. 2017; Li, Vasile,  
and Belta 2017; Camacho et al. 2019) have been used to  
specify behavior. Though these methods can be more ex-  
pressive, they often lead to intractable planning and learn-  
ing problems due to state-space explosion issues (Wong-  
piromsarn, Topcu, and Murray 2010). We offer a differ-  
ent expressibility–tractability tradeoff. Preference-based RL  
methods (Wirth et al. 2017; Brown et al. 2019) learn a re-  
ward function based on a dataset of preferences over tra-  
jectories. But, as we have argued, preferences over trajec-  
tory probabilities can be very difficult to specify. In addi-  
tion, our reward scheme relieves the need for environ-  
ment-specific preference datasets created by human experts.  
Multi-objective RL (Vamplew et al. 2011; Toro Icarte et al.  
2018) allows for different tasks to be specified through a  
set of reward functions. Our work proceeds in the orthog-  
onal direction by designing a single reward function to trade  
off among multiple behaviors, instead of incentivizing all of  
them.

Designing reward functions to increase the speed of learn-  
ing is a relatively open question. Mataric (1994) proposed to  
accelerate learning by incorporating domain knowledge and  
using a progress estimator, but does not provide a princi-  
pled method of designing a reward function. Sowerby, Zhou,

and Littman (2022) showed that reward functions that max-  
imize the action gap given a measure of horizon length lead  
to fast learning. However, designing such reward functions  
require detailed knowledge of the environment, making this  
approach impractical for new learning problems.

## 3 Problem Setting

We view an RL environment as a Markov Decision Pro-  
cess (MDP), with state space  $S$ , action space  $A$ , transi-  
tion model  $T$ , reward function  $R$ , and discount factor  $\gamma$ .  
A policy  $\pi : S \times A \rightarrow [0, 1]$  is a mapping from the cur-  
rent state to a probability distribution of the action to be  
taken. The optimal policy starting from some initial state  
 $s_0$  in the MDP is defined as any reward-maximizing pol-  
icy  $\pi^* \in \operatorname{argmax}_{\pi} \mathbb{E}[\sum_t \gamma^t r_t | s_0, \pi]$ . To make the reward-  
design problem as simple as possible for designers, we limit  
the reward function  $R : S \rightarrow \mathbb{R}$  to be defined solely on  
states. In goal–obstacle tasks, we consider the goal states  
and obstacle states to be absorbing.

We are interested in the reward-design problem. In the  
common RL framework, tasks are specified by the reward  
function and the agent’s objective is to maximize rewards.  
We take an alternative perspective: We specify tasks by pre-  
scribing a set of desirable policies and seek reward functions  
such that maximizing the reward will lead to the desirable  
policies. Formally, given a set of desirable (Pareto-optimal)  
policies  $\Pi$ , the reward-design problem is to create a reward  
function  $R : S \rightarrow \mathbb{R}$  such that the optimal policy  $\pi_R^* \in \Pi$ .

We imagine the state space  $S$  as exhibiting a tiered struc-  
ture, where higher tiers are more desirable than lower tiers,  
and states within the same tier are equally desirable. We for-  
mally define a Tier MDP as:

**Definition 3.1.**  $k$ -Tier Markov Decision Process: A Tier  
MDP is an MDP with state space  $S$ , action space  $A$ , transi-  
tion model  $T : S \times A \times S \rightarrow \mathbb{R}$ , reward function  
 $R : S \rightarrow \mathbb{R}$ , and discount factor  $\gamma$ . The state space is  
partitioned into  $k$  tiers, where  $S = S_1 \cup S_2 \cup \dots \cup S_k$  and  
 $S_i \cap S_j = \emptyset, \forall i \neq j \in 1, 2, \dots, k$ . The reward function has  
the form  $R(s) = r_i, \forall s \in S_i, i = 1, 2, \dots, k$ . In addition,  
 $r_1 < r_2 < \dots < r_k$ .

As an example, the grid world from Russell and Norvig  
(2010), as illustrated in Figure 1, could be formulated as a  
3-Tier MDP—the goal state is one tier ( $S_3$ ), the lava state  
one tier ( $S_1$ ), and all other states reside in the background  
tier ( $S_2$ ). It is important to note that we put no constraints on  
how many states could be in each tier, nor how many tiers  
there can be. Therefore, the framework has a high degree

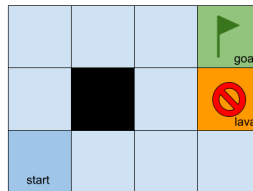


Figure 1: Russell/Norvig grid world. Objective is to reach  
the goal (green) without first visiting lava (red) ( $\gamma = 0.9$ ).

of generality; any finite MDP with reward defined on states could be formulated as a Tier MDP by placing states with the same reward in the same tier. However, the Tier MDP is most useful when there are clear good and bad states in the state space, such as when there are goal and obstacle states, or even states of intermediate desirability such as subgoal states. In the following sections, we will show how to perform reward design in Tier MDPs.

## 4 Policy Ordering

A policy can be thought of as inducing a probability distribution over an infinite set of outcomes (specifically the probability of reaching each of the states after  $t$  steps, for all  $t$ ). In goal-obstacle tasks, policies can be characterized by statistics such as probability of reaching the goal and probability of avoiding the obstacle for each possible horizon length.

For the moment, we limit the problem space to 3-Tier MDPs for simplicity, and generalize to  $k$ -Tier MDPs in Section 6. In a 3-Tier MDP, we will call the 3 tiers obstacles ( $S_1$ ), background ( $S_2$ ), and goals ( $S_3$ ), in order of increasing desirability. States in  $S_1$  and  $S_3$  are absorbing. We define  $o_t$  to be the probability of being in  $S_1$  at timestep  $t$ , and  $g_t$  that of  $S_3$ .

Given two policies  $\pi^A$  and  $\pi^B$ , we say  $\pi^A$  *dominates*  $\pi^B$  when both of these inequalities hold (and not both being strictly equal at all times):

$$\sum_{i=0}^t o_i^A \leq \sum_{i=0}^t o_i^B, \quad \forall t = 0, 1, 2, \dots, \infty,$$

$$\sum_{i=0}^t g_i^A \geq \sum_{i=0}^t g_i^B, \quad \forall t = 0, 1, 2, \dots, \infty.$$

In words, one policy dominates another if it gets to the goal faster, while delaying encountering obstacles longer. The set of policies that are not dominated by any other policy is the set of *Pareto-optimal* policies. Because there is a finite number of policies and domination is transitive, the set of Pareto-optimal policies is non-empty. We provide a visualization of Pareto-optimal policies in Appendix C.

Pareto-optimal policies are interesting to consider for two main reasons. First, Pareto-optimal behavior always exists, even when policies that achieve other reasonable things do not. Secondly, Pareto-optimality resolves the preference problem by defining a strict partial ordering over the entire policy space. Although the policies on the Pareto frontier are incomparable among themselves, they are all better than the set of Pareto-dominated policies. We simply deem the set of Pareto-optimal policies to be the desirable behavior, and all others undesirable. Next, we show how to design rewards that guarantee Pareto-optimal policies.

## 5 Tiered Reward

In this section, we seek a sufficient condition on the reward function so that optimizing expected discounted reward will always result in a Pareto-optimal policy with respect to our preference relation.

**Definition 5.1.** Pareto-optimal rewards: A reward function  $R(s)$  is called *Pareto-optimal* if the policy it induces,  $\pi_R \in \operatorname{argmax}_{\pi} \mathbb{E}[\sum_t \gamma^t r_t | s_0, \pi]$ , is Pareto-optimal.

Even some reasonable-sounding reward functions need not be Pareto-optimal. Going back to the Russell/Norvig grid example, an intuitive reward design would be requiring  $r_{lava} < r_{background} < r_{goal}$ . Consider three example reward functions in Table 1 that satisfy this constraint: Both  $R$  and  $G$  are Pareto-optimal, while  $B$  is Pareto-dominated (see Figure 10 in Appendix). Roughly,  $B$  doesn't encourage getting to the goal but is also not good at avoiding lava.

Policy	$r_{lava}$	$r_{background}$	$r_{goal}$
R	-1	-0.1	+1
G	-1	0	+0.5
B	-1	-0.9	0

Table 1: Three example reward functions of Russell/Norvig grid world.

In fact, many of the reward functions that satisfy  $r_{lava} < r_{background} < r_{goal}$  are not Pareto-optimal. Out of 1000 such rewards that we sampled randomly, 90.5% were Pareto-dominated (See Figure 13 in Appendix). Next, we present a simple rule that is sufficient to guarantee environment-independent Pareto-optimal reward functions in 3-Tier MDPs.

**Definition 5.2.** Tiered Reward: In a 3-Tier Markov Decision Process with discount factor  $\gamma \in (0, 1)$ , a reward function defined by

$$R(s) = \begin{cases} r_{obs} & \text{if } s \in S_1 \\ r_{background} & \text{if } s \in S_2 \\ r_{goal} & \text{if } s \in S_3 \end{cases}$$

is considered a *Tiered Reward* if

$$r_{obs} < \frac{1}{1-\gamma} r_{background} < r_{goal}.$$

and states in  $S_1$  and  $S_3$  are absorbing.

**Theorem 5.3** (Pareto-optimal rewards in 3-Tier MDP). *In a 3-Tier Markov Decision Process, a Tiered Reward is Pareto-optimal.*

We leave the proof in Appendix A but provide some intuition for Tiered Reward here. The middle term in Definition 5.2,  $\frac{1}{1-\gamma} r_{background}$ , is equal to the cumulative discounted return for infinitely getting a reward in the background tier ( $(1 + \gamma + \gamma^2 + \dots)r_{background}$ ). So, in a gross simplification, as long as the reward at the goal is more appealing than infinitely wandering in background states, and the obstacle less appealing, the reward induces behavior that arrives at the goal early and avoids the obstacles. Following this simple constraint, we as reward designers can easily create Pareto-optimal reward functions without requiring knowledge of the transition probabilities in the environment. Though environment-specific knowledge is needed partition the state space into tiers, Tiered Reward is generally applicable and environment-independent in the sense that the reward structure remain the same and the reward values for each tier are shared across different MDPs.

## 6 Generalizing to $k$ Tiers

In Sections 4 and 5, we limited the discussion to 3-Tier MDPs. But MDPs with more than 3 tiers can usefully model important problems such as those with well-defined subgoal states. Specifically, each subgoal region could be its own tier, instead of being grouped into one big background tier. Even though these problems could still be solved as a 3-Tier MDP, more knowledge about the environment could help design better reward functions and accelerate learning. So, in this section, we consider the reward-design problem in Tier MDPs with more than three tiers.

**Definition 6.1.** Tiered Reward: In a  $k$ -Tier ( $k > 3$ ) Markov Decision Process with discount factor  $\gamma \in (0, 1)$  where the goal tier ( $k$ ) is absorbing, the reward function  $R$  is a Tiered Reward if  $R(s) = r_i, \forall s \in S_i, i = 1, 2, \dots, k$ , for reward values  $r_1, r_2, \dots, r_k \in \mathbb{R}$ , that satisfy

$$r_1 < \left(\frac{1}{1-\gamma}\right)r_2 < \left(\frac{1}{1-\gamma}\right)^2 r_3 < \dots < \left(\frac{1}{1-\gamma}\right)^{k-1} r_k \leq 0.$$

Notice that the Tiered Reward in the  $k$  tiers case uses a stricter condition than that of 3 tiers. First, all reward values are non-positive. This is a sufficient but not necessary condition to guarantee Pareto-optimality. We enforce this constraint not only because of mathematical convenience (used later in Equation 1), but also because step-wise penalty has been proved to support faster learning (Koenig and Simmons 1993). Specifically, with a zero-initialized value function, step penalties create an incentive for the agent to try state-action pairs it has never experienced before, resulting in rapid exploration. Secondly, the reward values of higher tiers are exponentially greater than the lower ones. For adjacent tiers  $i$  and  $i + 1$ , The reward values always satisfy  $r_i < \frac{1}{1-\gamma} r_{i+1} < 0$ . One such reward is visualized in Figure 2.

This definition can be understood as a generalization of the 3-Tiered Reward. When the agent resides within tier  $i \in \{2, 3, \dots, k-1\}$ , the  $k$  tiers could be partitioned into 3 groups to construct a 3-Tier MDP. In particular,  $S_1$  will include tiers 1 through  $i - 1$ ,  $S_2$  is just tier  $i$ , and  $S_3$  is tiers  $i + 1$  to  $k$ . Note that we can generalize Theorem 5.3 to allow states in  $S_1$  and  $S_3$  to have any reward values as long as they satisfy the inequality in Definition 5.2 for a fixed reward value in  $S_2$ . Namely, denote  $r_{low} = \max\{r_1, \dots, r_{i-1}\}$  and  $r_{high} = \min\{r_{i+1}, \dots, r_k\}$ , and as a  $k$ -Tiered Reward they satisfy

$$r_{low} < \left(\frac{1}{1-\gamma}\right)r_i < \left(\frac{1}{1-\gamma}\right)^2 r_{high}$$

And since  $\gamma \in (0, 1)$ ,

$$r_{low} < \left(\frac{1}{1-\gamma}\right)r_i < \left(\frac{1}{1-\gamma}\right)^2 r_{high} \leq r_{high}. \quad (1)$$

That is,  $(r_{low}, r_i, r_{high})$  is a Tiered Reward function in the 3-Tier MDP with tiers  $S_1, S_2$ , and  $S_3$ , and therefore induces Pareto-optimal policies (Theorem 5.3). So, at tier  $i$ , the policy that optimizes the  $k$ -Tiered Reward will push agents to higher tiers as fast as possible and avoid lower tiers, as if they were goals and obstacles, respectively. In the special case that the agent resides within tier  $i = 1$ , the constraint

from Definition 6.1 will treat tiers 2 through  $k$  as if they are all goals, pushing the agent towards them. In the case that  $i = k$ , the agent is already in the ‘‘goal tier’’. So overall,  $k$ -Tiered Reward will induce in a ratchet-like policy—go to the higher tiers as fast as possible while not fall back to the lower tiers—that makes learning fast. In fact, it has been shown that a similar increasing reward profile (Sowerby, Zhou, and Littman 2022) leads to fast learning. Okudo and Yamada (2021) and Zhai et al. (2022) have also shown that intermediate rewards can accelerate learning and provably improve sample efficiency in goal-reaching tasks.

Besides encouraging early visitation of good tiers, using Tiered Reward also guarantees maximum total visitation of all good tiers. This property is formalized in Theorem 6.2.

**Theorem 6.2** (Tiered Reward and Cumulative Tier Visitation). *In a  $k$ -Tier Markov Decision Process that has Tiered Reward  $R(s)$ , the induced optimal policy is  $\pi^*$ . Let  $p_i^{*d} \in [0, 1]$  be the probability of being in tier  $d \in \{1, 2, \dots, k\}$  for the first time at timestep  $t$  following policy  $\pi^*$ . Then, there is no policy  $\pi$ , along with its induced probability distribution  $p_t^d$ , that satisfies both:*

$$\begin{aligned} \sum_{i=0}^t p_i^1 &\leq \sum_{i=0}^t p_i^{*1}, \quad \forall t = 0, 1, 2, \dots, \infty, \text{ and} \\ \sum_{i=0}^t p_i^d &\geq \sum_{i=0}^t p_i^{*d}, \quad \forall d = [2..k], \forall t = 0, 1, 2, \dots, \infty. \end{aligned}$$

The proof is similar to that of Theorem 5.3 and can be found in Appendix B. To state the theorem in words, if a  $k$ -Tier MDP has a Tiered Reward structure, then the resulting policy will visit the worst tier ( $S_1$ ) for as few times as possible, while visiting all the other good tiers ( $S_2, \dots, S_k$ ) as often as possible, respectively.

## 7 Experiments

In this section, we aim to verify the usefulness of our proposed Tiered Reward. We empirically show that Tiered Rewards are able to make learning faster on multiple tabular domains. We extend our results to environments with high-dimensional inputs and show that Tiered Reward works with deep RL algorithms. Finally, we also explore the influence of the number of tiers and find that having more tiers can induce faster learning.

### Fast Learning with Tiered Rewards

Guaranteeing Pareto-optimal behavior is not the sole benefit of using Tiered Rewards; we find that it also leads to fast learning. There are many ways to design a Tiered Reward because it is a class of reward functions that is only constrained by an inequality (Definition 6.1), and not by specific reward values. In this section, for simplicity and clarity we use  $k$ -Tiered Reward defined by:

$$r_i = \begin{cases} 0 & \text{if } i = k \\ \frac{1}{1-\gamma} r_{i+1} - \delta & \text{if } i < k \end{cases}$$

where  $\delta$  is a small constant used to satisfy the strict inequality constraint.

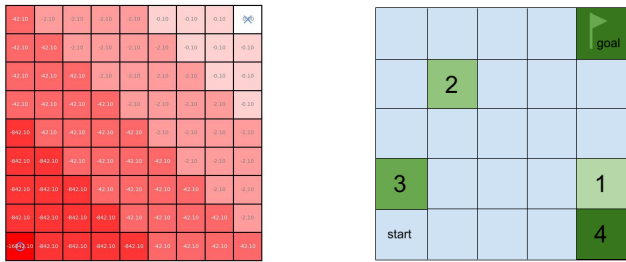


Figure 2: Left: A Tiered Reward in a grid world with 6 tiers. Start state is in the bottom left corner, goal state in top right. Darker colors correspond to more negative reward values. Right: Flag grid by Ng, Harada, and Russell (1999).

The “Flag Grid” from Ng, Harada, and Russell (1999) is a natural 6-Tier MDP to study Tiered Reward. In this grid world (Figure 2 right), the agent begins in the bottom-left corner and must learn to pick up four flags in sequence before reaching the goal. The state space is the location of the agent plus the flag it has collected. The agent can move in 4 directions with an 80% success rate, while acting randomly 20% of the time. All states in which the agent possesses the same number of flags constitute a tier, totaling 5 tiers. The goal constitutes the sixth and final tier.

To evaluate Tiered Reward, we compare it against two baseline reward functions. The first one, following Koenig and Simmons (1993), we call *action penalty*. This reward penalizes each step with  $-1$ , until the goal state is reached and the agent is awarded  $+1$ . To reiterate, such step-wise negative reinforcement encourages directed exploration. This reward only assumes knowledge about the position of the goal.

The Flag Grid domain was introduced in the context of potential-based shaping (Ng, Harada, and Russell 1999). In that work, the authors showed how knowledge of the sub-goals could be leveraged through shaping rewards to guide the learning process. Our Tiered Rewards can be used similarly, so we compare potential-based shaping to Tiered Rewards in this environment. For direct comparability, we use the Tiered Reward as a potential function  $\Phi(s) = R_{tier}(s)$  to shape the action-penalty reward, resulting in what we call *tier-based shaping reward*:  $R_{tbs}(s, a, s') = R_{penalty}(s) + \gamma\Phi(s') - \Phi(s)$ .

We compare these reward functions first in the context of Q-Learning (Watkins and Dayan 1992), arguably the most well-understood and widely applicable RL algorithm. As Figure 3 (top) shows, Tiered Reward always learns fastest of the three. Perhaps surprisingly, tier-based shaping reward performs orders of magnitudes worse than even action penalty. That is because, with discounting, the shaping function  $F(s, a, s') = \gamma\Phi(s') - \Phi(s)$  becomes positive when  $s$  and  $s'$  belong to the same tier. As a result, the zero-initialized Q-values are not optimistic with respect to these rewards, and so exploration with  $R_{tbs}$  is undirected, leading to slow learning. For a fairer comparison, we also plot the learning curves where all Q-values are initialized to some arbitrary large value so that  $R_{tbs}$  also enjoys directed exploration as

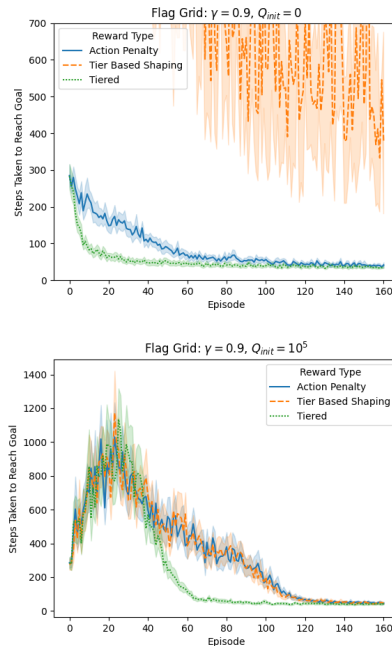


Figure 3: Q Learning curves for Flag Grid. The two plots use different initial Q-values. Each experiment was run with 30 seeds. We experimented with a range of discounts  $\gamma \in \{0.99, 0.95, 0.90, 0.85\}$  and found they all had similar performances, and only report  $\gamma = 0.90$  here.

the two other rewards (Figure 3, bottom). We tried different initialization values ( $10^{10}$ ,  $10^5$ ,  $10^3$ ) and observed similar results, so we only report  $Q_{init} = 10^5$  here. There is a noticeable spike in time taken to reach the goal early on during training. It is the result of optimistic Q-value initialization, which leads to more exploration and thus slower learning. Regardless of this trade off, Tiered Reward still consistently outperforms the two baselines.

It is important to note that our goal here is not to argue shaping is ineffective, nor to determine how to initialize Q-values for fast learning, but solely to demonstrate the usefulness of Tiered Reward in various different settings. To start, it makes learning faster than tier-based shaping reward and action penalty for different discount factors and Q-value initialization schemes. Moreover, it is simple to design and implement; there is no need to engineer environment-specific reward and initial Q-values to accelerate learning.

### Tiered Reward in Deep RL

We further show that Tiered Reward also make learning faster in Deep RL with image observations. We choose three goal—obstacle environments from MiniGrid (Chevalier-Boisvert et al. 2023):

1. EmptyGrid: a *visual* grid world ( $8 \times 8$ ) where the agent starts in one corner and aims for the opposite corner.
2. FourRooms: a *visual* grid world ( $19 \times 19$ ) where the agent must navigate to the goal (green) in one of four rooms by going through the gaps in the wall.

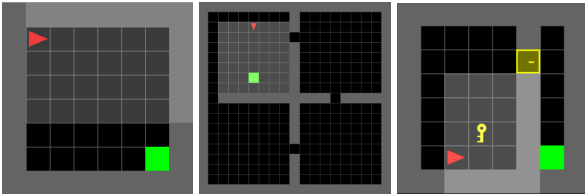


Figure 4: Illustration of EmptyGrid, FourRooms, and DoorKey from left to right. The agent is in red, and the goal in green. All three environments use visual observations.

3. DoorKey: a *visual* grid world ( $8 \times 8$ ) where the agent must first pick up a key, then travel to and unlock a door, and finally navigate to the goal.

In all three environments (Figure 4), the agent aims to learn a policy to navigate to the goal using image observations. FourRooms is a long-horizon problem; the DoorKey environment has a complicated transition function and action space, and is hard to solve using classical RL algorithms with a sparse reward. In all three environments, we design Tiered Reward with three tiers. For EmptyGrid and FourRooms, tiers are assigned based on each state’s  $L1$  distance to the goal; for DoorKey, tiers are assigned based on the sub-goals the agent has completed (getting key, opening door, and reaching goal).

We use Proximal Policy Optimization (Schulman et al. 2017) (PPO) as the RL algorithm, and use an ImpalaCNN (Espeholt et al. 2018) as the policy network architecture. More experiment details are included in Appendix E. To provide numerical stability, deep RL methods often employ reward scaling and clipping (Henderson et al. 2018). To follow, we linearly scale the tiered reward values to be between  $-1$  and  $0$ .

Following the previous set up, we compare Tiered Reward against action penalty and tier-based shaping. To evaluate the learning performance, we plot the episodic return during learning using the original reward function from MiniGrid (Chevalier-Boisvert et al. 2023). The original reward functions in MiniGrid are designed by human experts for each MiniGrid environment, and express the task of reaching the goal quickly and avoiding obstacles. By plotting the learned policy’s performance on the original reward function, we can examine how quickly the agent has learned the desired behavior. Figure 5 shows the learning performance of PPO on three environments. In all three, Tiered Reward is able to accumulate high episodic returns, thereby learning the desired behavior. Across the three environments, Tiered Reward show the fastest learning, outperforming the Action Penalty and Tier Based Shaping baselines. Tier Based Shaping performs differently according to how hard the exploration problem is: as discussed before, when  $s$  and  $s'$  are in the same tier, the shaping function  $F(s, a, s') = \gamma\Phi(s') - \Phi(s) > 0$ , and therefore encourages the agent to exploit rather than explore. For FourRooms, Tiered Reward initially learns slower than Tier Based Shaping, but later catches on and eventually outperforms its counterpart. All three reward functions suffer from large standard devi-

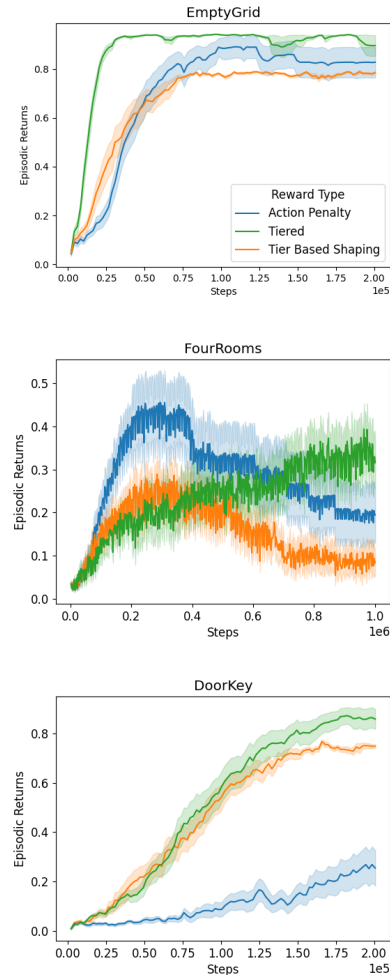


Figure 5: Learning curves of three reward functions on EmptyGrid, FourRooms, and DoorKey. Each agent is trained with the reward function labeled on the plot, but evaluated using the original MiniGrid reward ( $1 - 0.9 * \text{step count}/\text{max steps}$  for success, and  $0$  for failure). Error bars show standard deviation from 30 random seeds.

ation in this environment likely because this environment is a hard exploration problem; different exploration during learning leads to wildly different outcomes.

### Influence of More Tiers

Finally, we explore Tiered Reward with a varying number of tiers. First, we choose for simplicity and clarity four grid-world domains with absorbing goals and obstacles that are suited to a flexible number of tiers:

1. Chain: a 90-state 1D environment with left and right actions. Starting from one end, the agent tries to reach the other end with actions of success rate 80%; failed actions transition to the opposite direction.
2. Grid: a  $9 \times 9$  grid where the agent starts in one corner and aims for the opposite corner. The agent can move in



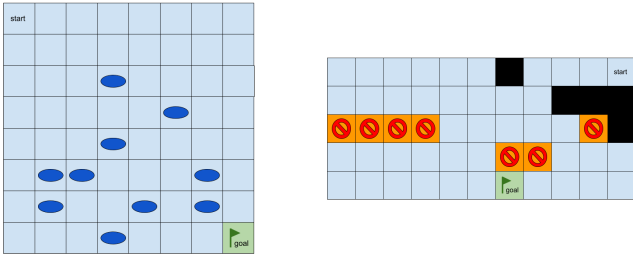


Figure 6: Left: Frozen lake environment with holes in dark blue. Right: Wall Grid environment with walls in black and lava in orange.

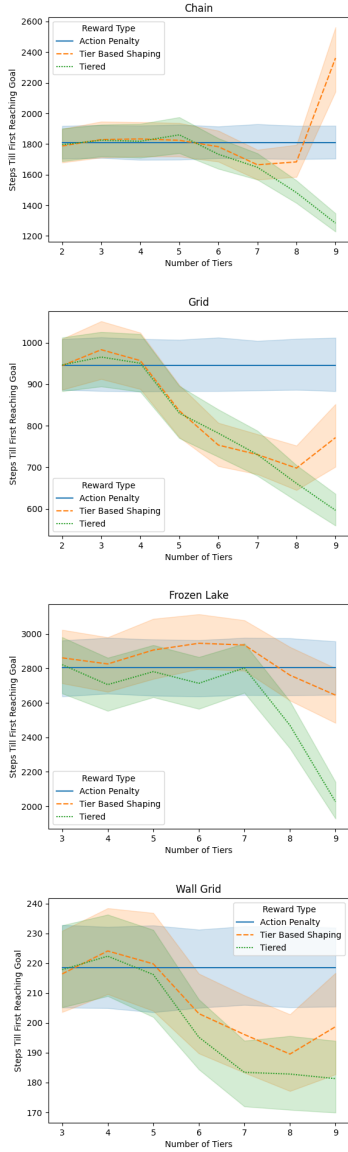


Figure 7: Q-Learning results with  $\gamma = 0.9$ . Each experiment was run with 300 seeds.

four cardinal directions with a 80% success rate, while slipping to either side with a 10% chance.

3. Frozen Lake: a slippery grid with holes that will swallow the agent (Figure 6 left). The objective is to reach the goal without falling into any holes. Each of the 4 directional actions succeed 1/3 of the time, and slip to either side with probability 1/3.
4. Wall Grid: a grid world with multiple lava states and wall states (Figure 6 right). The agent has to circle around the walls while avoiding the lava to get to the goal. Transition dynamics same as Grid.

For Chain and Grid, tiers are decided based on their  $L1$  distance to the goal; for Frozen Lake and Wall Grid, tiers are assigned based on the sum of  $L1$  distance to the goal and start state, weighted 2 : 1. Since there are 3 types of states in the latter two environments, we start at 3 tiers instead of 2.

In absence of a “correct” reward function that expresses the tasks, we measure the learning speed by recording the steps required for the agent to reach the goal for the first time. For fair comparison, we optimistically initialize  $Q_{init} = 10^5$  so that  $R_{tbs}$  also enjoys the benefit of directed exploration. The results are presented in Figure 7. We repeat the same experiments with a model-based RL algorithm, RMAX (Brafman and Tenenholz 2002). The results are similar to that of Q-learning (Figure 11 in Appendix F). As expected, Tiered Reward makes learning faster as the number of tiers increases because more information about the environment aids reward design. Tiered Reward consistently beats action penalty and is at least as good as tier-based shaping reward, and often much better. Even when Tiered Reward performs the same as shaped reward, it provides the added benefit of simplicity and better interpretability—it is based only on states, and not state–action–state triples.

Adding more tiers is more complicated in deep RL settings because scaling the reward values to  $[-1, 0]$  for learning stability in deep RL will decrease the difference of reward value among tiers, especially among higher tiers. Figure 8 shows the learning performance of Tiered Reward with 3, 5, 7, and 9 tiers on EmptyGrid, FourRooms, and DoorKey. In EmptyGrid, having more tiers makes learning faster and more stable. In DoorKey, 7 and 9 tiers produce similar results, both significantly faster than 3 or 5 tiers. In FourRooms, 5 tier leads to the fastest learning result, and using more than 5 tiers monotonically decreases learning performance. We believe this is because of numerical issues during scaling of Tiered Reward: reward values for all states in tiers higher than 3 gets normalized to very close to 0 (in the range  $10^{-6}$  to  $10^{-15}$ ), and therefore tiers become indistinguishable under some numerical accuracy. Having more tiers suffers more from this problem because more states become indistinguishable<sup>1</sup>. We hypothesize that this issue can be resolved with a smarter reward scaling or clipping method, and leave that for future work. In practice, the optimal number of tiers can be determined empirically or a priori with MDP-specific information. Though more tiers sometimes leads to

<sup>1</sup>To alleviate the numerical issues caused by scaling, we set discount factor to 0.5 in these experiments to obtain smaller original Tiered Reward. See Appendix H for further details

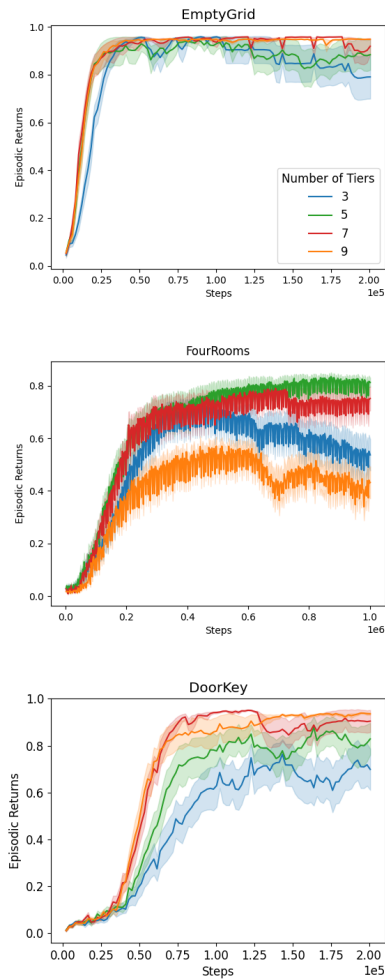


Figure 8: Learning curves on EmptyGrid, FourRooms, and DoorKey with different number of tiers in Tiered Reward. Error bars show standard deviation from 30 random seeds.

slower learning than 3 tiers, they all provide faster learning than the two reward baselines in Figure 5.

## 8 Conclusion

In contrast to standard reward-design solutions that are environment-dependent, we presented Tiered Rewards—a class of environment-independent reward functions that provably leads to (Pareto) optimal behavior and empirically leads to fast learning. Tiered Reward can be defined in both tabular and high dimensional environments, and is RL-algorithm agnostic. One interesting future work is getting theoretical guarantees that Tiered Reward lead to asymptotically faster learning.

## References

Abel, D.; Dabney, W.; Harutyunyan, A.; Ho, M. K.; Littman, M.; Precup, D.; and Singh, S. 2021. On the expressivity of

markov reward. *Advances in Neural Information Processing Systems*, 34: 7799–7812.

Amodei, D.; and Clark, J. 2016. Faulty reward functions in the wild. URL: <https://blog.openai.com/faulty-reward-functions>.

Amodei, D.; Olah, C.; Steinhardt, J.; Christiano, P.; Schulman, J.; and Mané, D. 2016. Concrete problems in AI safety. *arXiv preprint arXiv:1606.06565*.

Brafman, R. I.; and Tenenbholz, M. 2002. R-MAX—A General Polynomial Time Algorithm for Near-Optimal Reinforcement Learning. *Journal of Machine Learning Research*, 3: 213–231.

Brown, D.; Goo, W.; Nagarajan, P.; and Niekum, S. 2019. Extrapolating beyond suboptimal demonstrations via inverse reinforcement learning from observations. In *International conference on machine learning*, 783–792. PMLR.

Camacho, A.; Chen, O.; Sanner, S.; and McIlraith, S. A. 2017. Non-markovian rewards expressed in LTL: guiding search via reward shaping. In *Tenth annual symposium on combinatorial search*.

Camacho, A.; Icarte, R. T.; Klassen, T. Q.; Valenzano, R. A.; and McIlraith, S. A. 2019. LTL and Beyond: Formal Languages for Reward Function Specification in Reinforcement Learning. In *IJCAI*, volume 19, 6065–6073.

Chevalier-Boisvert, M.; Dai, B.; Towers, M.; de Lazcano, R.; Willems, L.; Lahlou, S.; Pal, S.; Castro, P. S.; and Terry, J. 2023. Minigrid. *CoRR*, abs/2306.13831.

Devidze, R.; Radanovic, G.; Kamalaruban, P.; and Singla, A. 2021. Explicable reward design for reinforcement learning agents. *Advances in Neural Information Processing Systems*, 34: 20118–20131.

Espeholt, L.; Soyer, H.; Munos, R.; Simonyan, K.; Mnih, V.; Ward, T.; Doron, Y.; Firoiu, V.; Harley, T.; Dunning, I.; et al. 2018. Impala: Scalable distributed deep-rl with importance weighted actor-learner architectures. In *International conference on machine learning*, 1407–1416. PMLR.

Henderson, P.; Islam, R.; Bachman, P.; Pineau, J.; Precup, D.; and Meger, D. 2018. Deep reinforcement learning that matters. In *Proceedings of the AAAI conference on artificial intelligence*, volume 32.

Ho, M. K.; Correa, C. G.; and Ritter, D. 2021. Models of Sequential Decision Making (msdm).

Icarte, R. T.; Klassen, T.; Valenzano, R.; and McIlraith, S. 2018. Using reward machines for high-level task specification and decomposition in reinforcement learning. In *International Conference on Machine Learning*, 2107–2116. PMLR.

Icarte, R. T.; Klassen, T. Q.; Valenzano, R.; and McIlraith, S. A. 2022. Reward machines: Exploiting reward function structure in reinforcement learning. *Journal of Artificial Intelligence Research*, 73: 173–208.

Koenig, S.; and Simmons, R. G. 1993. Complexity analysis of real-time reinforcement learning. In *AAAI*, volume 93, 99–105.

Li, X.; Vasile, C.-I.; and Belta, C. 2017. Reinforcement learning with temporal logic rewards. In *2017 IEEE/RSJ*



*International Conference on Intelligent Robots and Systems (IROS)*, 3834–3839. IEEE.

Littman, M. L.; Topcu, U.; Fu, J.; Isbell, C.; Wen, M.; and MacGlashan, J. 2017. Environment-independent task specifications via GLTL. *arXiv preprint arXiv:1704.04341*.

Mataric, M. J. 1994. Reward functions for accelerated learning. In *Machine learning proceedings 1994*, 181–189. Elsevier.

Mornati, F. 2013. Pareto Optimality in the work of Pareto. *Revue européenne des sciences sociales. European Journal of Social Sciences*, (51-2): 65–82.

Ng, A. Y.; Harada, D.; and Russell, S. 1999. Policy invariance under reward transformations: Theory and application to reward shaping. In *Icml*, volume 99, 278–287.

Okudo, T.; and Yamada, S. 2021. Subgoal-based reward shaping to improve efficiency in reinforcement learning. *IEEE Access*, 9: 97557–97568.

Russell, S. J.; and Norvig, P. 2010. *Artificial Intelligence (A Modern Approach)*.

Schulman, J.; Wolski, F.; Dhariwal, P.; Radford, A.; and Klimov, O. 2017. Proximal policy optimization algorithms. *arXiv preprint arXiv:1707.06347*.

Sowerby, H.; Zhou, Z.; and Littman, M. L. 2022. Designing Rewards for Fast Learning.

Sutton, R. S.; and Barto, A. G. 1998. *Reinforcement Learning: An Introduction*. The MIT Press.

Toro Icarte, R.; Klassen, T. Q.; Valenzano, R.; and McIlraith, S. A. 2018. Teaching multiple tasks to an RL agent using LTL. In *Proceedings of the 17th International Conference on Autonomous Agents and MultiAgent Systems*, 452–461.

Vamplew, P.; Dazeley, R.; Berry, A.; Issabekov, R.; and Dekker, E. 2011. Empirical evaluation methods for multiobjective reinforcement learning algorithms. *Machine Learning*, 84(1): 51–80.

Watkins, C. J.; and Dayan, P. 1992. Q-learning. *Machine learning*, 8(3): 279–292.

Wirth, C.; Akrou, R.; Neumann, G.; Fürnkranz, J.; et al. 2017. A survey of preference-based reinforcement learning methods. *Journal of Machine Learning Research*, 18(136): 1–46.

Wongpiromsarn, T.; Topcu, U.; and Murray, R. M. 2010. Receding horizon control for temporal logic specifications. In *Proceedings of the 13th ACM international conference on Hybrid systems: computation and control*, 101–110.

Zhai, Y.; Baek, C.; Zhou, Z.; Jiao, J.; and Ma, Y. 2022. Computational benefits of intermediate rewards for goal-reaching policy learning. *Journal of Artificial Intelligence Research*, 73: 847–896.

## A Proof of Theorem 5.3

*Proof.* Let  $\pi^*$  be the optimal policy induced with Tiered Reward  $R(s)$ . Suppose, for the sake of contradiction, there exists some policy  $\pi$  that dominates  $\pi^*$ . Then, by our definition of Pareto dominance,

$$\begin{aligned} \sum_{i=0}^t o_i &\leq \sum_{i=0}^t o_i^*, \quad \forall t = 0, 1, 2, \dots, \infty, \\ \sum_{i=0}^t g_i &\geq \sum_{i=0}^t g_i^*, \quad \forall t = 0, 1, 2, \dots, \infty, \end{aligned}$$

where  $o_t$  and  $g_t$  are the probabilities of reaching obstacles and goals in exactly  $t$  steps following  $\pi$ , and  $o_t^*$  and  $g_t^*$  are the same for  $\pi^*$ . We can write the value function (of  $\pi$  being evaluated on  $R(s)$ ) as

$$V = \sum_{t=0}^{\infty} g_t (\gamma^t r_{goal} + \sum_{j=0}^{t-1} \gamma^j r_{back}) + o_t (\gamma^t r_{obs} + \sum_{j=0}^{t-1} \gamma^j r_{back}).$$

The value of  $\pi^*$  ( $V^*$ ) can be written similarly. Denote

$$\begin{aligned} f_t^g &= \gamma^t r_{goal} + \sum_{j=0}^{t-1} \gamma^j r_{back}, \text{ and} \\ f_t^o &= \gamma^t r_{obs} + \sum_{j=0}^{t-1} \gamma^j r_{back}. \end{aligned}$$

That is,  $f_t^g$  is the reward obtained on a trajectory that reaches a goal in  $t$  steps and  $f_t^o$  is the reward obtained on a trajectory that reaches an obstacle in  $t$  steps. With  $r_{obs} < \frac{1}{1-\gamma} r_{back} < r_{goal}$ , we show below that  $f_t^g$  is strictly decreasing and  $f_t^o$  strictly increasing with respect to  $t$ .

Proof that  $f_t^g$  is strictly decreasing:

$$\begin{aligned} f_{t+1}^g - f_t^g &= \gamma^{t+1} r_{goal} + \sum_{j=0}^t \gamma^j r_{back} - \gamma^t r_{goal} - \sum_{j=0}^{t-1} \gamma^j r_{back} \\ &= \gamma^t (\gamma - 1) r_{goal} + \gamma^t r_{back} \\ &= \gamma^t (1 - \gamma) \left( \frac{1}{1 - \gamma} r_{back} - r_{goal} \right) \\ &< 0 \end{aligned}$$

because  $0 < \gamma < 1$  and  $\frac{1}{1-\gamma} r_{back} < r_{goal}$ .

Proof that  $f_t^o$  is strictly increasing:

$$\begin{aligned} f_{t+1}^o - f_t^o &= \gamma^{t+1} r_{obs} + \sum_{j=0}^t \gamma^j r_{back} - \gamma^t r_{obs} - \sum_{j=0}^{t-1} \gamma^j r_{back} \\ &= \gamma^t (\gamma - 1) r_{obs} + \gamma^t r_{back} \\ &= \gamma^t (1 - \gamma) \left( \frac{1}{1 - \gamma} r_{back} - r_{obs} \right) \\ &> 0 \end{aligned}$$

because  $0 < \gamma < 1$  and  $r_{obs} < \frac{1}{1-\gamma} r_{back}$ .

Then,

$$\begin{aligned} V - V^* &= \sum_{t=0}^{\infty} (g_t - g_t^*) f_t^g + \sum_{t=0}^{\infty} (o_t - o_t^*) f_t^o \\ &= \sum_{t=0}^{\infty} \left( \sum_{j=0}^t g_j - g_j^* \right) (f_t^g - f_{t+1}^g) + \sum_{t=0}^{\infty} \left( \sum_{j=0}^t o_j - o_j^* \right) (f_t^o - f_{t+1}^o) \quad (*) \\ &> 0 + 0 \\ &= 0. \end{aligned}$$

The pass from the first equality to the second (\*) is justified as follows:

$$\begin{aligned}
\sum_{t=0}^{\infty} (g_t - g_t^*) f_t^g &= \sum_{t=0}^{\infty} \sum_{j=0}^t (g_j - g_j^*) f_t^g - \sum_{t=0}^{\infty} \sum_{j=0}^{t-1} (g_j - g_j^*) f_t^g \\
&= \sum_{t=0}^{\infty} \sum_{j=0}^t (g_j - g_j^*) f_t^g - \sum_{t=1}^{\infty} \sum_{j=0}^{t-1} (g_j - g_j^*) f_t^g \\
&= \sum_{t=0}^{\infty} \sum_{j=0}^t (g_j - g_j^*) f_t^g - \sum_{t'=0}^{\infty} \sum_{j=0}^{t'} (g_j - g_j^*) f_{t'+1}^g \\
&= \sum_{t=0}^{\infty} \left( \sum_{j=0}^t g_j - g_j^* \right) (f_t^g - f_{t+1}^g)
\end{aligned}$$

Similarly,

$$\sum_{t=0}^{\infty} (o_t - o_t^*) f_t^o = \sum_{t=0}^{\infty} \left( \sum_{j=0}^t o_j - o_j^* \right) (f_t^o - f_{t+1}^o)$$

We have shown, through the value function, that  $\pi$  is strictly better than  $\pi^*$  with respect to the reward function  $R$ . But  $\pi^*$  was chosen to optimize  $R$ , so that's a contradiction. Since no such  $\pi$  can exist, that means  $\pi^*$  is not dominated by any policy, and is therefore Pareto-optimal.  $\square$

## B Proof of Theorem 6.2

*Proof.* The proof is similar to that of Theorem 5.3. Suppose, for the sake of contradiction, that there exists some such policy  $\pi$ . We can express the value functions as

$$V = \sum_{t=0}^{\infty} \gamma^t \sum_{m=1}^k r_m \cdot p_t^m, \text{ and}$$

$$V^* = \sum_{t=0}^{\infty} \gamma^t \sum_{m=1}^k r_m \cdot p_t^{*m}.$$

Denote  $f_t^m = \gamma^t r_m$ . Then,  $f_t^m - f_{t+1}^m = r_m \gamma^t (1 - \gamma) \leq 0, \forall m$ . It's easy to see  $f_t^m - f_{t+1}^m$  is strictly increasing in  $m$ , so

$$\begin{aligned} V - V^* &= \sum_{t=0}^{\infty} \gamma^t \sum_{m=1}^k r_m (p_t^m - p_t^{*m}) \\ &= \sum_{m=1}^k \sum_{t=0}^{\infty} f_t^m (p_t^m - p_t^{*m}) \\ &= \sum_{m=1}^k \sum_{t=0}^{\infty} (f_t^m - f_{t+1}^m) \left( \sum_{j=0}^t p_j^m - p_j^{*m} \right) \\ &> \sum_{m=1}^k \sum_{t=0}^{\infty} (f_t^1 - f_{t+1}^1) \left( \sum_{j=0}^t p_j^m - p_j^{*m} \right) \quad (**) \\ &= \sum_{t=0}^{\infty} (f_t^1 - f_{t+1}^1) \sum_{m=1}^k \left( \sum_{j=0}^t p_j^m - p_j^{*m} \right) \\ &= \sum_{t=0}^{\infty} (f_t^1 - f_{t+1}^1) \cdot \sum_{j=0}^t \left( \sum_{m=1}^k p_j^m - \sum_{m=1}^k p_j^{*m} \right) \\ &= \sum_{t=0}^{\infty} (f_t^1 - f_{t+1}^1) \cdot \sum_{j=0}^t (1 - 1) \\ &= 0 \end{aligned}$$

Note that the (\*\*) step is justified only because  $\sum_{j=0}^t p_j^m - p_j^{*m} \geq 0, \forall m = [2..k], \forall t$ . The inequalities show that  $\pi$  achieves higher reward than the optimal policy, which is a contradiction. No such  $\pi$  exists.  $\square$

## C Visualization of Pareto-optimal Policies

Going back to the example of the Russell/Norvig grid, we can visualize how the probability of reaching the goal ( $g_t$ ) and reaching lava ( $o_t$ ) changes over time for different policies. Consider two simple policies on the Russell/Norvig grid—(1) going left from all states (“always left”) and (2) going right from all states (“always right”).

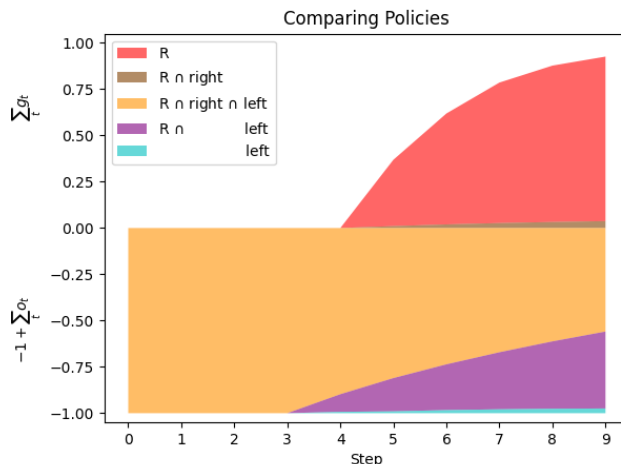


Figure 9: Visualization of the policies of always going left and always going right in the (stochastic) Russell/Norvig grid. The policy  $R$  is the same as  $R$  in Figure 10. To avoid color overlapping, we separated each policy into disjoint regions visualized by distinct colors. Each colored region in the figure represent the probability-region of one or more policies, joined by  $\cap$ . For example, the policy “always right” covers the areas in brown and orange.

We visualize each policy as a shaded area upper bounded by  $\sum_t g_t$  and lower bounded by  $-1 + \sum_t o_t$  in Figure 9. This visualization can be understood as separating the probability space into two, with the goal-reaching probability on the top half of the y-axis in  $[0, 1]$  and obstacle-hitting probability in the bottom half of the y-axis in  $[-1, 0]$ . With this visualization, a Pareto-dominated policy will cover an area that is entirely enclosed by that of a dominating policy because of lower goal-reaching probabilities on the top half and higher obstacle-hitting probabilities on the bottom half. As Figure 9 shows, “always right” and “always left” do not cover each other, so they are incomparable. Specifically, “always right” has a slightly higher probability of reaching the goal (brown), but “always left” has a lower probability of reaching the lava (purple and teal).

For comparison, we plot another policy, which we call  $R$ , that is state-dependent and moves in the direction of the goal. For policy  $R$ , the probability of reaching the target increases with time because each step has a 20% slip probability; agents could slip early on and take longer to reach the goal. Note that area covered by  $R$  (red, brown, orange, and purple) completely subsumes that of “always right” (brown and orange), demonstrating that “always right” is dominated by  $R$ . “Always left”, on the other hand, is not dominated by  $R$  because it has a lower probability of reaching lava (teal). However, “always left” is not Pareto-optimal of course, because it is dominated by policy  $G$  in Table 1.

In Figure 10, we visualize the three policies  $R$ ,  $G$ , and  $B$  in Table 1. Both  $R$  and  $G$  are Pareto-optimal, while  $B$  is Pareto-dominated because  $B$ ’s areas are entirely enclosed by that of  $R$  and of  $G$ .



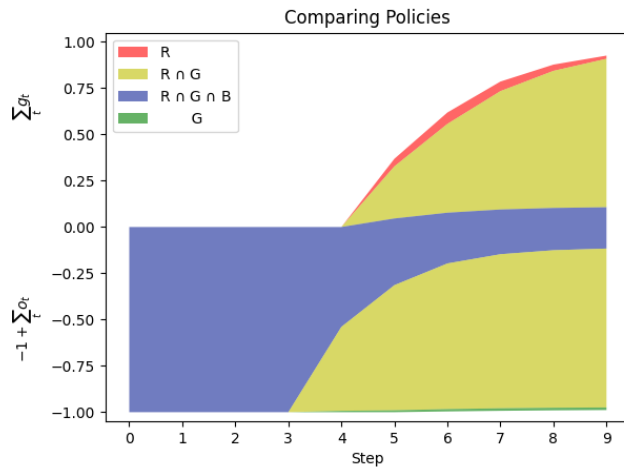


Figure 10: Visualization of three different policies (R, G, B) on Russell/Norvig grid. Visualization scheme is the same as described in Figure 9.

## D Tabular Grid Worlds Experiment Details

The implementation of many tabular environments and algorithms is based on the MSDM library by Ho, Correa, and Ritter (2021). All MSDM experiments are run on an Ubuntu 18.04 system with an Intel Core i7-9700K CPU and 32G of RAM.

Following Koenig and Simmons (1993), we use a greedy policy for action selection and initialize the Q-values optimistically to exploit directed exploration. Since all reward values are non-positive, it is sufficient to initialize the Q-values to 0. We use a learning rate of  $\alpha = 0.90$  (tuned from  $\alpha \in \{0.95, 0.90, 0.85\}$ , all of which performed similarly). We set the small constant  $\delta = 0.1$ .

## E MiniGrid Experiment Details

The DeepRL experiments on MiniGrid environment were run on an Ubuntu 18.04 system using a single 6GB GPU (NVIDIA GeForce GTX 980 Ti) and took between 40-60min per seed, depending on the environment.

A Proximal Policy Optimization (PPO) agent was trained on the three MiniGrid environments using the following hyperparameters:

Hyperparameter	Parameter Value	Note
Epochs	4	
Batch Size	256	
Learning Rate ( $\alpha$ )	$1 \times 10^{-3}$	
Total Env Steps	200000	Total training steps in each environment
Discount Factor ( $\gamma$ )	0.5	See Appendix H
Small Constant ( $\delta$ )	5	Used to satisfy the strict inequality in Tiered Reward
GAE $\lambda$	0.95	$\lambda$ coefficient in the GAE formula
Entropy Coefficient	0.01	
Value Loss Coefficient	0.5	
Max Grad Norm	0.5	Maximum norm of gradient
Clipping $\epsilon$	0.2	

Table 2: PPO hyperparameters on MiniGrid experiments.

The PPO agent used an ImpalaCNN architecture for the policy and value network. The architecture of the policy network is as follows:

Layer Name	Layer Type	Output Dimension
Conv Sequence 1	Convolutional Layers	16
Conv Sequence 2	Convolutional Layers	32
Conv Sequence 3	Convolutional Layers	32
Hidden Layer	Linear Layer	256
Logit Layer	Linear Layer	256
Value Layer	Linear Layer	256

Table 3: Architecture of the policy network of the Proximal Policy Optimization agent used in MiniGrid experiments.

Each Conv Sequence in Table 4 is a sequence of convolutional and pooling layers with residual connections. Each convolutional and pooling layer in the conv sequence has the same number of output channels, as specified in the output dimension in Table 4. The architecture of a Conv Sequence is as follows:

Layer #	Layer Type	Kernel Size	Stride	Padding
1	Conv	3	1	1
2	Max Pool	3	2	1
3	Relu			
4	Conv	3	1	1
5	Relu			
6	Conv	3	1	1
7	Relu			
8	Conv	3	1	1
9	Relu			
10	Conv	3	1	1

Table 4: Architecture of a Conv Sequence.

There are two residual connections: one between layers 3 and 6, and another between layers 7 and 10.

## F RMAX results

We set maximal reward  $r_{max} = 10^5$ , use the first  $m = 3$  transition samples to model the MDP (tuned from  $m \in \{2, 3, 5, 7, 10\}$  and selected based on good resulting policy while taking similar learning time to Q-Learning), and did 200 iterations of value iteration during each update.

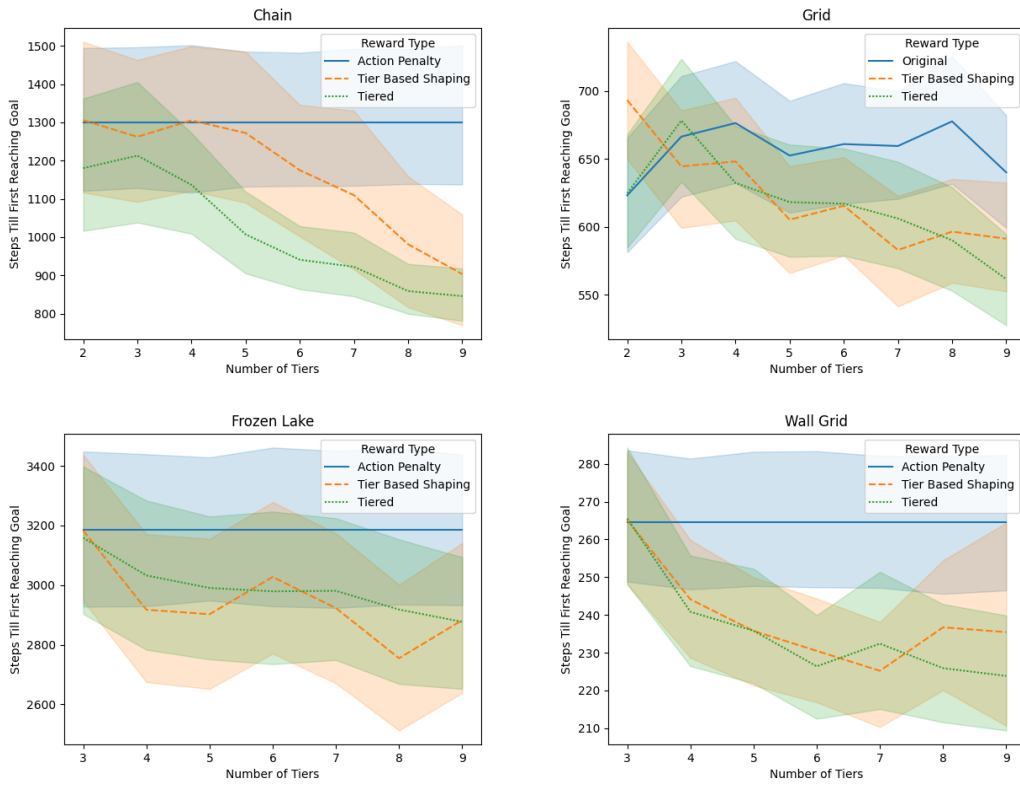


Figure 11: RMAX results with  $\gamma = 0.9$ . Each experiment was run with 300 seeds.

## G Visualizing Additional Tiers on Empty Grid

To aid the understanding of Tiered Reward, we provide below visualizations of Tiered Reward on a grid world with different number of Tiers. In this grid world, the agent starts at the bottom right corner, and the goal is the top left corner. We assign the tiers based on a state's  $L_1$  distance to the goal.

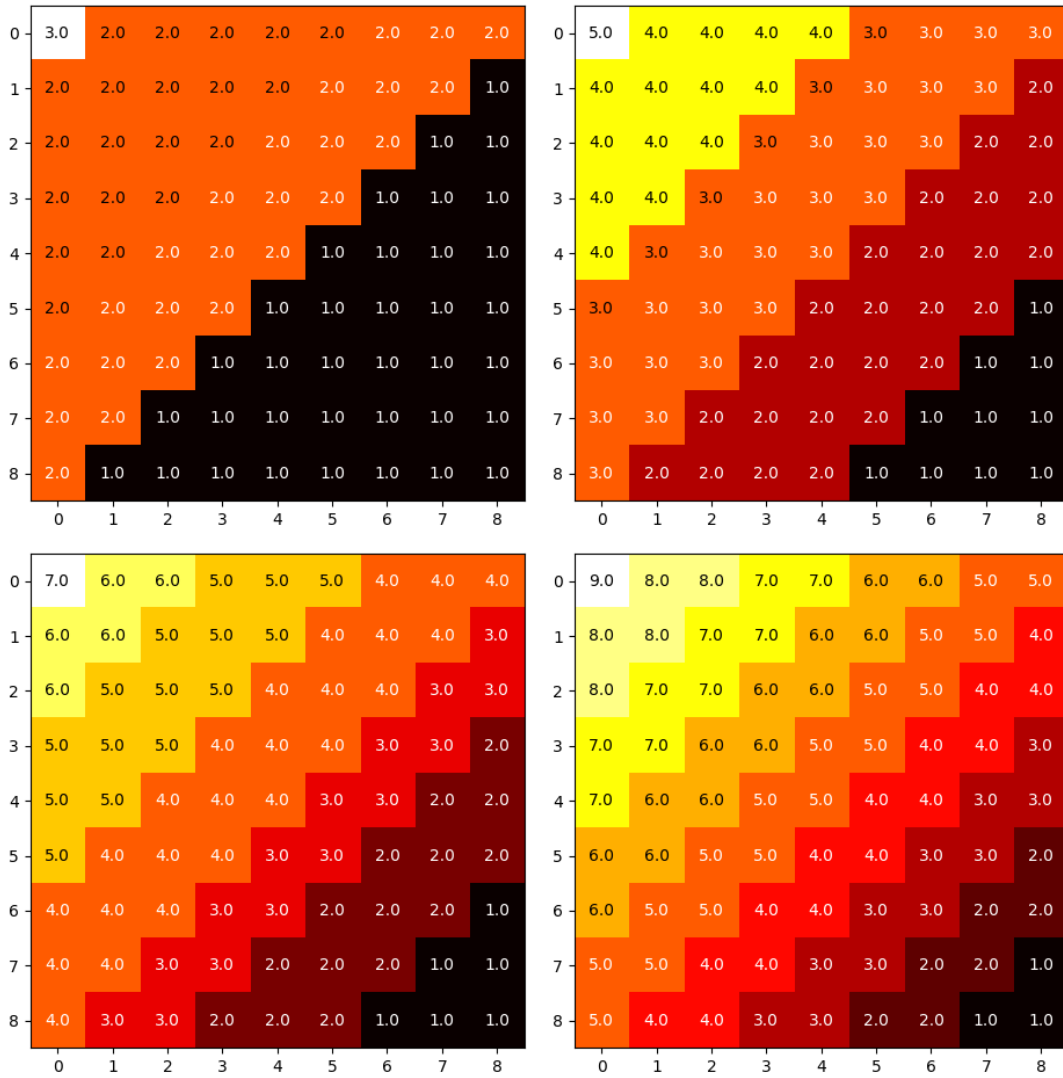


Figure 12: A visualization of Tiered Reward for 3 (top left), 5 (top right), 7 (bottom left), and 9 (bottom right) tiers on a grid world. Each color in the plot represents one single tiers, and the numbers represent the tier number.



## H Scaled Tiered Reward for Different Tiers

We provide here the numerical values of the Tiered Reward after scaling it to be between  $[-1, 0]$ . This provides intuition on how using smaller discount values can reduce the numerical problems during reward scaling because big values of  $\gamma$  (for example,  $\gamma = 0.99$  or  $\gamma = 0.9$ ) will make scaled reward values numerically equal for different tiers, especially the higher tiers.

	Tier	$\gamma = 0.99$	$\gamma = 0.5$
Tiered Reward	5	0	0
	4	-5	-5
	3	-505	-15
	2	-50505	-35
	1	-5050505	-75
Scaled Tiered Reward	5	0	0
	4	$-9.9 \times 10^{-7}$	-0.06
	3	$-9.9 \times 10^{-5}$	-0.2
	2	$-9 \times 10^{-3}$	-0.4667
	1	-1	-1

Table 5: Comparing scaled and unscaled reward values using a total of 5 tiers and  $\delta = 5$ . Reward values for two discount factors ( $\gamma$ ) are provided.

	tier	$\gamma = 0.99$	$\gamma = 0.5$
Tiered Reward	9	0	0
	8	-5	-5
	7	-505	-15
	6	-50505	-35
	5	-5050505	-75
	4	-505050505	-155
	3	-50505050505	-315
	2	-5050505050505	-635
	1	-505050505050505	-1275
Scaled Tiered Reward	9	0	0
	8	$-9 \times 10^{-15}$	-0.0039
	7	$-9 \times 10^{-13}$	-0.0118
	6	$-9 \times 10^{-11}$	-0.2258
	5	$-9 \times 10^{-9}$	-0.0588
	4	$-1 \times 10^{-6}$	-0.1216
	3	$-9 \times 10^{-5}$	-0.2471
	2	-0.01	-0.4980
	1	-1	-1

Table 6: Comparing scaled and unscaled reward values using a total of 9 tiers and  $\delta = 5$ . Reward values for two discount factors ( $\gamma$ ) are provided.

## I Additional Figures

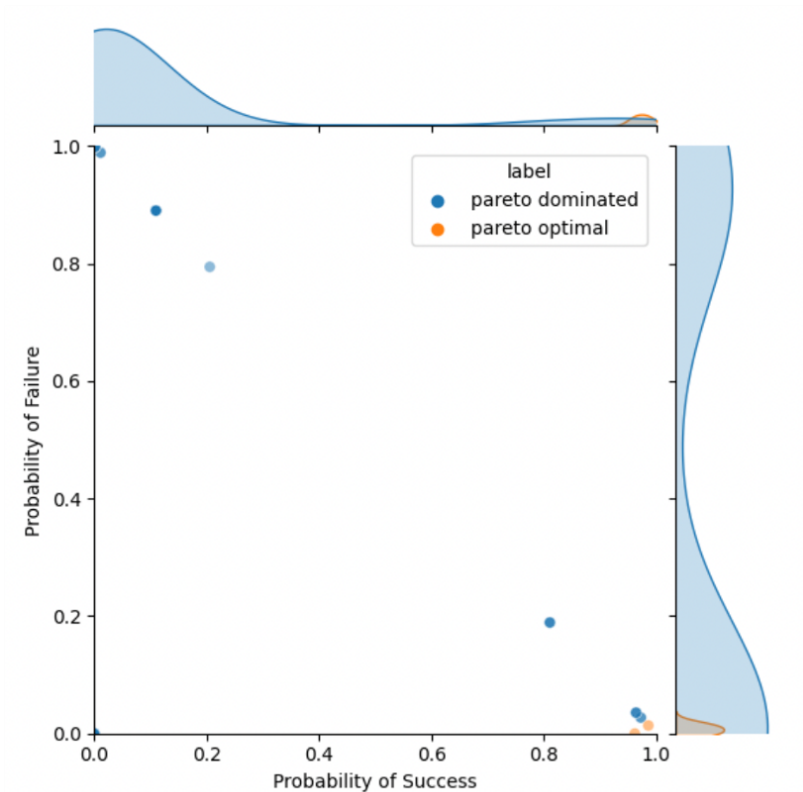


Figure 13: 1000 policies that are induced by random reward functions that satisfy  $r_{lava} < r_{back} < r_{goal}$  from the Russell/Norvig grid. Each point in the scatter plot represents one policy's probability of success (reaching the goal) and failure (reaching the lava), showing that the majority (90.5%) of policies in the policy space are Pareto-dominated.